JOURNAL OF CATALYSIS **139**, 119–133 (1993)

Carbon–Carbon Bond Formation via Aldolization of Acetaldehyde on Single Crystal and Polycrystalline TiO_2 Surfaces

H. IDRISS,[1] K. S. KIM,[2] AND M. A. BARTEAU[3]

Center for Catalytic Science and Technology, Department of Chemical Engineering,
University of Delaware, Newark, Delaware 19716

Received February 12, 1992; revised July 10, 1992

The aldol condensation of acetaldehyde, CH_3CHO, to form crotonaldehyde, $CH_3CH{=}CHCHO$, and crotyl alcohol, $CH_3CH{=}CHCH_2OH$, takes place on single-crystal surfaces of TiO_2 (rutile), even under ultrahigh-vacuum conditions. Both the {011}-faceted TiO_2(001) surface (which nominally exposes only fivefold coordinated cations) and the {114}-faceted (001) surface (which exposes four-, five-, and sixfold coordinated cations) are active for this bimolecular reaction. This observation is in contrast to the sharp activity difference between these two surfaces for carboxylate ketonization and suggests that aldol condensation does not exhibit a strong dependence on surface structure. The principal reaction observed in TPD and XPS experiments to compete with aldolization of acetaldehyde was reduction to ethanol; Cannizzaro disproportionation to acetate plus ethoxides and reductive coupling to butene were minor pathways. The aldolization selectivity increased somewhat as the surface heterogeneity increased from the {011}-faceted TiO_2(001) surface, to the {114}-faceted (001) surface, and to polycrystalline TiO_2 (anatase) powder. This selectivity variation likely reflects the influence of surface heterogeneity on the activity for the various competing reactions, especially hydrogenation; the aldol coupling reaction, although bimolecular, appears to be relatively insensitive to surface structure. © 1993 Academic Press, Inc.

INTRODUCTION

The chemistry of oxygen-containing reagents on surfaces of metal oxides is the basis of catalytic processes as varied as selective oxidation, alcohol synthesis, reduction, condensation, etherification, and gasoline production from methanol. The selectivities in such processes lie in the details of the oxide properties, the nature of the surface–adsorbate interaction, and the process conditions. Important characteristics of solid oxide catalysts which influence reactivity include acid–base properties, redox properties, and surface structures. The richness of this chemistry has motivated numerous studies of the catalytic reactivity of oxides. Among the studies of oxygenates on oxide surfaces, both single crystals and powders, one can find those of carboxylic acids (*1–4*), alcohols (*5–8*), aldehydes (*9–11*), ketones (*11–13*), and esters (*14–15*). Aldehydes, in particular, are among the most versatile probe reagents because of their ability to form C–C bonds by condensation, in addition to the possibility of their oxidation to carboxylic acids (*16*) and reduction to alcohols (*17*). Aldehyde reactions observed on oxide surfaces include Cannizzaro-type reactions (*18, 19*), condensation reactions (*11, 20–23*), selective reduction (*17*), selective oxidation (*16*), acetal formation (*23*), and carbonyl metathesis (*24*). An examination of the chemistry of the simplest aldehyde, formaldehyde, reveals that these reactions often do not occur cleanly. For example, the Cannizzaro reaction of formaldehyde to formate and methoxide species has been observed on different oxides including TiO_2 (*18*), ThO_2 (*18*), CeO_2 (*19*),

---

[1] Present address: SABIC, P.O. Box 5101, Riyadh 11422, Saudi Arabia.

[2] Present address: Yukong Ltd., Ulsan Research Center, P.O. Box 4, Ulsan, Kyung-Nam, South Korea.

[3] To whom correspondence should be addressed.

0021-9517/93 $5.00

$ZnAl_2O_4$ (*25*) powders, and MgO(100) (*26*) and TiO_2(001) (*27*) single crystals. Direct oxidation of formaldehyde to formates competes with this reaction on $ZnAl_2O_4$ powders, leading to an excess of surface formates (*25*). Direct reduction to methoxides occurs on reduced, defective TiO_2(001) single-crystal surfaces (*27*) producing an excess of methoxides on the surface; this excess decreases on more oxidized surfaces of the same single crystal. The MgO(100) surface is highly selective for the Cannizzaro reaction, forming equal amounts of methoxides and formates from formaldehyde (*26*). The ZnO(0001) surface is more selective for simple oxidation of formaldehyde to formates as expected for a more easily reduced material (*28*). These results clearly indicate that formaldehyde reaction and decomposition on oxide surfaces, even single crystals, is complex and may depend critically on the nature of the oxide and its pretreatment (especially with regard to oxidation/reduction).

The chemistry of higher aldehydes is potentially even more complex. Formaldehyde cannot undergo the aldolization reaction because it does not contain α-hydrogens (*29*). However, aldol condensation reactions of C_{2+} saturated and unsaturated aldehydes commonly occur on different oxides. It has been reported that titania powder catalyzes aldolization of C_3 and C_4 saturated aldehydes to produce C_6 and C_8 α,β-unsaturated aldehydes with high yields (*30*). Other oxides also catalyze self- and cross-aldolization of aldehydes and ketones; active materials include MgO (*31*, *32*), CaO (*31*, *32*), La_2O_3 (*31*), ZrO_2 (*31*), Sn/SiO_2 (*33*), and Al_2O_3 (*34*). We have recently observed aldolization of acetaldehyde with high selectivity to crotonaldehyde and crotyl alcohol on other oxides such as CeO_2, mixed Fe (II, III) oxides, and Cr_2O_3 (*35*), during TPD experiments on powders at atmospheric pressure. The fact that aldolization can be catalyzed in basic as well as in acidic environments (*36–38*) to yield higher α,β-unsaturated compounds makes this C–C bond-forming reaction an interesting probe of heterogeneous catalytic systems.

The presence of other reaction channels, such as direct reduction and direct oxidation, Cannizzaro and Tischenko reactions, reductive coupling, can divert the chemistry to other products. For example, on a TiO_2(001) single-crystal reduced by argon ion bombardment, we have observed that C_{2+} aldehydes undergo reductive coupling to form symmetric olefins (*24*). Surface oxidation would be expected to decrease reductive coupling, possibly promoting aldolization. However, oxidized surfaces may also favor the Cannizzaro reaction, which would produce acetates and ethoxides from acetaldehyde, for example. These intermediates can also lead to higher carbon-number products; we have observed that acetates (formed by acetic acid dissociation) produce acetone in a structure-sensitive reaction on the {114}-faceted structure of the TiO_2(001) surface (*2*). Given the complexity of this chemistry, it is essential to examine these reactions on well-defined surfaces under well-defined conditions in order to unravel the network of coupling reactions and the influence of surface structure and composition on these. In an effort to understand the reactions of higher aldehydes and to compare them to those of formaldehyde (*27*), temperature-programmed desorption (TPD) and X-ray photoelectron spectroscopy (XPS) studies of acetaldehyde were carried out on the two stable faceted structures of a TiO_2(001) single-crystal surface, as well as on titania powder (anatase). The {011}-faceted structure of the TiO_2(001) surface was obtained by annealing the sputtered surface to ca. 750 K for 20 min and the {114}-faceted structure was obtained by annealing the {011}-faceted surface to ca. 950 K for 20 min (*2*). Both faceted structures contain titanium cations in their highest (+4) oxidation states (*39*). All Ti^{4+} cations are fivefold coordinated in the {011}-faceted structure, while they are four-, five-, and sixfold coordinated in the {114}-faceted structure (*40*). Results from these single-crystal surfaces were compared with those from a TiO_2 (anatase) powder, which presumably contains all the site types (and likely a number of others) occurring on the single-crystal samples.

EXPERIMENTAL

Single-Crystal Experiments

TPD experiments were conducted in a stainless-steel, ion-pumped ultrahigh-vacuum chamber, Physical Electronics Model 548, described previously (*2, 6*). The UHV system was equipped with a single-pass cylindrical mirror analyzer for AES, four-grid LEED optics, and a quadrupole mass spectrometer for monitoring gaseous products. A cylindrical quartz envelope enclosed the ionizer of the mass spectrometer probe in order to minimize stray desorption from the sample mounting hardware. The envelope had an aperture of smaller diameter than that of the front face of the sample located at the end of the ionizer. Two additional openings were placed on each side of the envelope to facilitate pumping. The mass spectrometer was multiplexed with an IBM personal computer used for data acquisition in TPD experiments and for subsequent data manipulation. A typical TPD experiment was begun by dosing the sample at room temperature with acetaldehyde. After dosing, the chamber was pumped down until a stable background pressure was reached, typically ca. 5×10^{-10} Torr; the sample was then positioned in front of the mass spectrometer. Heating was initiated (1.2 K/s) and the desorption flux was monitored with the mass spectrometer. As many as 50 masses were scanned simultaneously as a function of temperature during a single TPD experiment. XPS experiments were conducted in a VG Scientific ESCALAB, described previously (*26*), equipped with a twin-anode X-ray source, ultraviolet lamp, LEED optics, electron and ion guns, and a UTI mass spectrometer also multiplexed with an IBM personal computer.

The (001)-oriented TiO_2 single-crystal sample ($10 \times 9 \times 1.5$ mm) was prepared from a rutile single-crystal boule (99.99%, Atomergic Chemetals Corp.). The crystal was aligned to within 0.5° of the (001) plane by the Laue method. After installation in the vacuum chamber the sample was cleaned by repeated cycles of argon ion bombardment (2 keV Ar^+ beam/20 min) and annealing (30 min at 900–950 K). The clean sample exhibited an AES O(510 eV)/Ti(380 eV) peak-to-peak ratio of ca. 1.65–1.70, typical of a fully oxidized TiO_2 single-crystal surface (*2, 39, 40*). AES measurements were conducted using a 2-keV electron beam. The electron beam was defocused on the sample at a beam current of 0.1 μA to avoid surface reduction caused by electron beam damage.

The TiO_2 sample was mounted by means of a sample holder made of tantalum foil (0.127 mm thick), which was described previously (*26*). Cooling of the sample was achieved via conduction by contacting the sample holder assembly with a liquid nitrogen reservoir. The lowest temperature that could be reached with this sample mount in the VG ESCALAB was 250 K; the C(1*s*) spectrum after acetaldehyde adsorption at 170 K was obtained with the PHI Model 550 system described previously (*2*). The sample temperature was monitored in all cases by means of a chromel–alumel thermocouple attached to the side of the sample using high-temperature cement (Aremco Ultra-Temp 516). AES and XPS measurements showed that no migration of the cement occurred during heat treatment of the sample throughout the experiments (*2, 6*).

Acetaldehyde was contained in a glass sample tube attached to the dosing manifold. Prior to use, acetaldehyde was cleaned by freeze–pump–thaw cycles. The reactant vapors were dosed onto the single-crystal sample through variable leak values equipped with stainless-steel dosing needles.

A typical XPS experiment consisted of an initial exposure of the sample using the same procedure as that for the TPD experiments. After pump down, the sample was positioned under the X-ray source and the spectrum was collected. For all spectra the C(1*s*), O(1*s*), and Ti(2*p*) regions were scanned. For experiments in which XPS spectra were collected as a function of temperature, the first set in the series was collected as described above; the sample was then heated to the desired temperature and allowed to cool to the original dosing temperature before additional spectra were collected. All TPD and XPS data illustrated were obtained following saturation exposures of acetaldehyde (ca. 2–3 langmuir based on measurement of the uncorrected chamber pressure during direct dosing, i.e., with the crystal in front of the dosing needle).

Titania Powder Experiments

Titania (anatase) powder was obtained from American Instrument Co. (BET surface area 10.3 m^2/g; its properties were previously described in detail (*7*)). Titania powder (100 mg) was placed on a fritted glass disk support (1.5 mm length, 10 mm diameter) within a quartz reactor and was pretreated in He at 773 K for 2 h (flow rate 30 ml/min). A quadrupole mass spectrometer operating at a pressure of ca. 10^{-7} Torr was used for product detection. The mass spectrometer chamber was connected to the flow reactor system by an atmospheric pressure sampling module (APSM) from UTI, which decreased the pressure to the operating range of the quadrupole. An IBM personal computer was used for data acquisition. The pretreated TiO$_2$ sample was exposed at room temperature to acetaldehyde vapor (ca. 400 Torr at 4°C) in He flow (30 ml/min) until saturation. After dosing, the sample was purged with a flow of He at 30 ml/min for 1 h. The reactor was then heated (30 K/min) at the same He flow rate to 850 K. As many as 50 masses could be sampled every 2–3 s with the multiplexed UTI 100 C mass spectrometer.

The saturation exposure of acetaldehyde on the powder sample was determined by adjusting the mass spectrometer to *m/e* 29 (the most abundant cracking fragment of acetaldehyde) and monitoring the signal while bypassing the reactor. After stabilization of the signal, the flow of acetaldehyde vapor in He was passed through the reactor and a sharp decrease of the signal was observed, indicative of uptake by the sample. After 3–5 min, depending on the amount of catalyst, the *m/e* 29 signal in the gas stream returned to its original value, indicative of surface saturation.

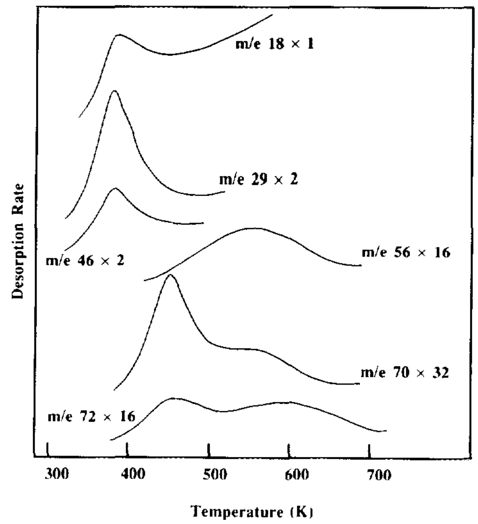

FIG. 1. Product desorption (uncorrected for mass spectrometer sensitivity) after acetaldehyde adsorption at room temperature on the {011}-faceted TiO$_2$(001) single crystal (the 750 K-annealed surface).

RESULTS

TPD of Acetaldehyde from the TiO$_2$(011)–{011}-Faceted Surface

TPD of acetaldehyde from the 750 K-annealed TiO$_2$(001) surface provided clear evidence for carbon–carbon bond formation beginning at temperatures as low as 400 K. Figure 1 presents the desorption spectra for representative mass fragments after acetaldehyde adsorption at room temperature. Three reaction channels are evident. The first at ca. 370–380 K consisted of water, acetaldehyde (CH$_3$CHO, *m/e* 29, 44), and ethanol (CH$_3$CH$_2$OH, *m/e* 46, 45, 31). The second channel, at 440 K, contained higher molecular wieght products identified as crotonaldehyde ($CH_3CH{=}CHCHO$, *m/e* 70) and crotyl alcohol ($CH_3CH{=}CHCH_2OH$, *m/e* 72). A third channel, at ca. 550 K, produced traces of butene ($CH_3CH{=}CHCH_3$, *m/e* 56, 41) in addition to small amounts of crotonaldehyde and crotyl alcohol.

The appearance of significant yields of products with masses greater than that of the reactant acetaldehyde provides clear evidence for association reactions on the surface. Before considering the quantitative analysis of the product distribution, it is worthwhile to consider, based on qualitative inspection of the TPD data, potential higher molecular weight products that can be omitted from further consideration. First, the signal for *m/e* 60 was negligible throughout the temperature range examined; thus the oxidation of acetaldehyde to acetic acid can be immediately ruled out. This conclusion is entirely consistent with our previous single-crystal and powder experiments with aldehydes and alcohols, which demonstrated the absence of oxidation activity of TiO_2 in the absence of gas-phase oxygen (*6*, *7*). Second, there was no evidence for the parent mass (*m/e* 88, 87), which would correspond to $CH_3CH(OH)CH_2CHO$, the product of simple aldol coupling (without further reaction) of acetaldehyde. Likewise there was no detectable signal for *m/e* 132 corresponding to the cyclic trimer, trimethyl trioxane, which has been reported on some metal surfaces (*41*).

The principal reaction products of acetaldehyde on the $TiO_2(001)$–{011}-faceted surface correspond to the following net reactions:

ethanol: reduction
crotonaldehyde: aldol condensation, dehydration
crotyl alcohol: aldo condensation, dehydration, reduction
butene: reductive coupling.

The relative yields of all carbon-containing products are listed in Table 1. These values were calculated from the TPD spectra of individual mass fragments as follows:

TABLE 1

Product Distribution for Acetaldehyde TPD on the {011}-Faceted Surface

Product	Fractional yield	Peak temperature (K)
Water	—	370–380
Acetaldehyde (*m/e* 29 : 2.3)[a]	0.30	370–380
Ethanol (*m/e* 31 : 2.1)	0.36	370–380
Butene (*m/e* 56 : 2.5)	0.01	550–570
Crotonaldehyde (*m/e* 70 : 5.6)	0.15	450
Crotonaldehyde	0.04	550–570
Crotyl alcohol (*m/e* 72 : 22)	0.03	450
Crotyl alcohol	0.11	550–570
Total C(1*s*) area	1.43 eV/ms[b]	Room temperature

[a] Mass spectrometer correction factor.

[b] C(1*s*) peak area from XPS after acetaldehyde adsorption at room temperature.

1. The peaks at 380, 440, and 560 K were separated and the area under each was obtained by numerical integration.
2. The experimentally determined fragmentation pattern for ethanol was scaled to account for the entire *m/e* 31 signal at 380 K and subtracted from the peak area of each mass at this temperature.
3. The remainder of the 380 K peak was accounted for by scaling the acetaldehyde cracking pattern to account for the remainder of the *m/e* 29 signal.
4. The fragmentation pattern for crotyl alcohol was scaled to account for all of the *m/e* 72 signal at 440 K and subtracted from the distribution.
5. The remainder of the 440 K peak was accounted for by scaling the crotonaldehyde fragmentation pattern to match the remaining signal for *m/e* 70.
6. The peak areas at 560 K were analyzed in the same fashion as those of the 440 K peak; the remainder of the signal for *m/e* 41 (after subtraction of the contributions from crotonaldehyde and crotyl alcohol) and the entire *m/e* 56 signal were assigned to butene.
7. Relative yields of each product were determined from the above scaling factors using mass spectrometer sensitivity factors (listed in Table 1) calculated by the method of Ko *et al.* (*42*). There were put on a percentage total carbon basis, shown in Table

1, by normalizing with respect to the carbon number of each product. The RMS percentage error (percentage of the mass spectrometer signal, positive or negative, for each mass remaining at the end of the analysis) was 5.7%, based on the 14 most abundant masses.

As shown in Table 1, only 30% of the acetaldehyde molecules initially adsorbed desorbed intact, 36% were hydrogenated to ethanol, and 34% were coupled to form the C_4 products crotonaldehyde and crotyl alcohol. These high yields of aldol condensation products from aldehydes on the $TiO_2(001)$–{011}-faceted surface are in sharp contrast to the negligible yields of bimolecular ketonization products from carboxylic acids on this surface. The ketonization reaction requires Ti^{4+} cations with pairs of coordination vacancies (*2*), a requirement met by the {114}-faceted but not by the {011}-faceted surface. Thus, it is apparent from Fig. 1 alone that bimolecular coupling of aldehydes via aldolization does not exhibit the same dependence on surface structure as the bimolecular ketonization of carboxylates; i.e., aldolization does not appear to be a structure-sensitive reaction.

TPD of Acetaldehyde on the $TiO_2(001)$–{114}-faceted Surface

TPD spectra for acetaldehyde desorption from a $TiO_2(001)$ surface previously annealed at 950 K (Fig. 2) were qualitatively similar to those for the 750 K-annealed surface (Fig. 1). There were several surprising differences, however. On the 950 K-annealed surface peaks for acetaldehyde, crotonaldehyde and crotyl alcohol converged to a common shape and 400 K peak temperature, in contrast to the ca. 60 K separation on the 750 K-annealed surface.

Quantitative analysis of the product distribution revealed further similarities and differences between the two surfaces. The conversion of acetaldehyde was similar in both cases, 70% on the 750 K-annealed surface versus 61% on the 950 K surface, but the selectivity to the aldol condensation products on the 950 K surface was nearly double that on the 750 K-annealed surface (see Table 2). The increase in aldol condensation selectivity came at the expense of acetaldehyde hydrogenation; ethanol, the dominant product on the 750 K surface, was

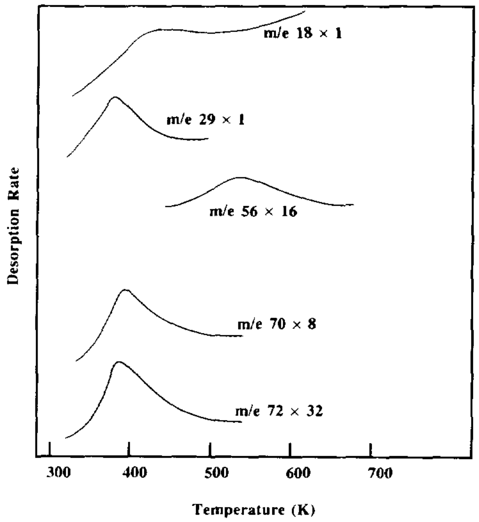

FIG. 2. Product desorption (uncorrected for mass spectrometer sensitivity) after acetaldehyde adsorption at room temperature on the {114}-faceted $TiO_2(001)$ single crystal (the 950 K-annealed surface).

TABLE 2

Product Distribution for Acetaldehyde TPD on the {114}-Faceted Surface

Product	Fractional yield	Peak temperature (K)
Acetaldehyde	0.39 (0.10)[a]	400
Ethanol	Traces	400
Butene	0.02 (0.005)	ca. 550
Crotonaldehyde	0.20 (0.05)	400
Crotyl alcohol	0.39 (0.10)	400
Total C(1*s*) XPS	0.38 eV/ms[b]	Room temperature

[a] Fractional yield normalized to total C(1*s*) area (i.e., multiplied by the ratio the of C(1*s*) area observed on this surface to that observed on the {011}-faceted surface (Table 1)).

[b] Peak area of the C(1*s*) spectrum after acetaldehyde adsorption at room temperature.

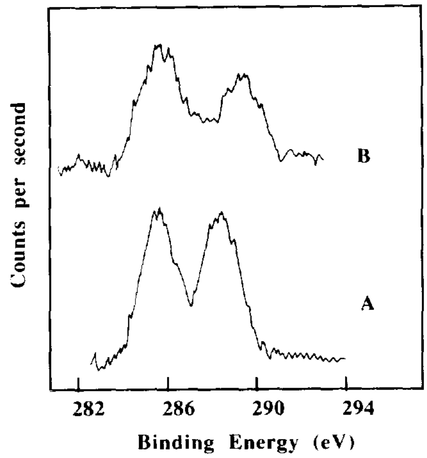

FIG. 3. C(1*s*) spectrum following acetaldehyde adsorption at 170 K on the surface of (A) the 750 K-annealed surface of the $TiO_2(001)$ single crystal and (B) the ZnO(0001) single crystal (from Ref. (*44*)).

essentially undetectable in acetaldehyde TPD from the 950 K-annealed surface. The origins of this selectivity shift are considered below. However, it should be noted that although the *selectivity* to aldol condensation products on the 950 K-annealed surface was twice that on the 750 K-annealed surface, the absolute *yield* of these products was actually about half that on the 750 K-annealed surface, as the total carbon coverage (determined from XPS experiments, discussed below) was reduced by a factor of 4 from the 850 K- to the 950 K-annealed surface. Regardless of whether one chooses to emphasize the selectivity increase or the yield decrease, the ×2 variation of aldol products is clearly much less than the order of magnitude difference in carboxylate ketonization activity between these two surfaces, and one may again conclude that aldolization is relatively structure-insensitive.

XPS Results

The results of surface spectroscopies provide further insights into the identity of the adsorbed intermediates that give rise to the complicated product slate noted above. Figure 3A presents the C(1*s*) spectrum obtained after acetaldehyde adsorption at 170 K on the surface of the {011}-faceted $TiO_2(001)$ single crystal. All spectra on titania were referenced to the $Ti(2p_{3/2})$ peak for Ti^{4+} at 459.3 eV; Ti^{4+} was the only oxidation state of titanium cations present at this surface (*2*, *27*). Two overlapping C(1*s*) peaks of nearly equal intensity were observed at 288.5 and 285.8 eV following acetaldehyde adsorption; these peaks can be assigned to the carbonyl carbon and methyl carbon of adsorbed acetaldehyde species, respectively. The separation of these peaks, 2.7 eV, is in good agreement with that for gaseous aldehydes (*43*) and the FWHM of each peak is 2.0 eV, close to the value expected for a single surface species. For comparison, the C(1*s*) spectrum of acetaldehyde at 170 K on the ZnO(0001) surface, obtained with the same spectrometer, is presented in Fig. 3B (this spectrum is taken from Ref. (*44*)). Two peaks centered at 285.8 and 289.2 eV were observed. While the lower binding-energy peak is in the same position as that observed on the $TiO_2(001)$ surface and attributed to the CH_3 group (Fig. 3A), the higher binding-energy peak (at 289.2) is in the region typical of carboxylates (*2*). Indeed, this result agrees well with the difference in reactivity of the two oxide single crystals: while formaldehyde and acetaldehyde were completely oxidized on the ZnO(0001) surface to formates (*28*) and acetates (*10*), only a small portion of these aldehydes produced carboxylates on any of the $TiO_2(001)$ surfaces examined (*27*).

Figure 4 presents the C(1*s*) spectra obtained after acetaldehyde adsorption on the $TiO_2(001)$–{011}-faceted surface at 260 K and as a function of annealing temperature. Two principal differences are apparent between the spectrum obtained after adsorption at 260 K (Fig. 4a) and that obtained at 170 K (Fig. 3A). The "carbonyl" peak at ca. 288.5 eV decreased significantly in intensity relative to the "alkyl" peak at ca. 286 eV in the 260 K spectrum. Moreover, the latter peak in the 260 K spectrum is considerably broader (>3 eV) than peaks obtained for

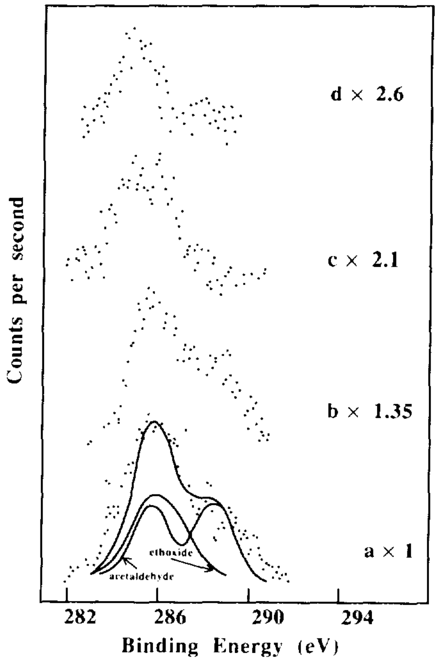

FIG. 4. C(1*s*) spectrum of acetaldehyde on the surface of the {011}-faceted TiO_2(001) single crystal as a function of reaction temperature. (a) 260 K, (b) surface in (a) heated to 310 K, (c) surface in (b) heated to 450 K, (d) surface in (c) heated to 600 K. Contributions to the spectrum in (a) from adsorbed acetaldehyde and ethoxide species, and the sum of these, are noted by the continuous curves.

adlayers containing a single type of organic species (<2 eV) (*2*, *27*, *45*). Thus in addition to unreacted acetaldehyde, the adsorbed layer must contain at least one other species which makes a large contribution to the C(1*s*) signal in the 285–287 eV range. This is precisely the contribution expected from adsorbed ethoxide species; we have previously shown that the ethoxide adlayer produced by ethanol dissociation on this surface is characterized by a broad peak, ca. 3 eV wide, centered at 285.9 eV (*45*). This ethoxide peak can be curve-fit with two overlapping peaks of nearly equal intensity, at 286.5 eV ($-CH_2O-$) and 285.3 eV (CH_3-). Although the adlayer at 260 K is clearly dominated by acetaldehyde and ethoxide species, the breadth of the peak envelope in Fig. 4a suggests that other species are also present. For example, if the entire intensity at 288.5 eV were assigned to the carbonyl group of acetaldehyde, there should be little intensity at 290 eV and above, as in Fig. 3A. That this is not the case suggests the presence of small amounts of a species with C(1*s*) binding energy higher than that of the acyl carbon of the aldehyde. The functional group that fits this description is the carboxyl group; surface acetates on TiO_2 give rise to a C(1*s*) peak at 289.5 eV (*2*). It is clear, however, that this group is a minor contributor to the C(1*s*) spectrum in Fig. 4a and therefore that the extent of the Cannizzaro reaction to form equal amounts of acetate and ethoxide species must be quite small. Thus the principal route to formation of ethoxides from acetaldehyde must be direct reduction rather than Cannizzaro-type disproportionation.

A similar inspection of the low-binding-energy side of the peak envelope suggests that small amounts of adsorbed carbon may also be present and contribute to the C(1*s*) intensity in this region of the spectrum (at ca. 284.1 eV). Complete decomposition of a small fraction of the adsorbed acetaldehyde would be expected to deposit atomic carbon and to provide the hydrogen consumed by ethoxide formation. The one surface species that can be ruled out, in spite of the broad C(1*s*) envelope in Fig. 4a, is the enolate (CH_2-CH-O). The C(1*s*) binding energy for the terminal CH_2 group in $CH_2C(CH_3)O$ ligands on ZnO is 283.7 eV (*13*). A peak at this binding energy with a typical FWHM of 2 eV is not compatible with the position of the leading edge of the C(1*s*) envelope (with negligible intensity below 283 eV) in Fig. 4a.

Heating the crystal to 310 K, Fig. 4b, resulted in a decrease of the surface population of carbon-containing species in general, with no significant differences in peak positions. By 450 K (Fig. 4c) the majority of species had desorbed (a small increase in carbon deposition was also observed); only traces of alkoxides at ca. 286.0 eV were still present. These results support those ob-

TABLE 3

Product Distribution for Acetaldehyde TPD on the Titania (Anatase) Powder

Product	Fractional yield	Peak temperature (K)
Acetaldehyde	0.20	380
Butadiene (*m/e* 54 : 3.8)[a]	0.05	500–600
Crotonaldehyde	0.68	430
Crotyl alcohol	0.07	450–460

[a] Mass spectrometer correction factor.

tained from TPD experiments which showed that ca. 80% of the carbon-containing products desorbed below 450 K (Table 1). At 600 K (Fig. 4d) 6% of the original C(1*s*) signal remained at the position (284.1 eV) for atomic carbon, indicating that essentially all molecular products had desorbed from the surface.

Adsorption of acetaldehyde at room temperature on the {114}-faceted surface, Fig. 5a, gave rise to a C(1*s*) envelope similar in shape to that obtained from the {011}-faceted surface: both spectra exhibit maximum intensity at ca. 285–286 eV, with extended "tails" or "shoulders" at higher binding energies. Careful inspection of the 310 K spectra in Figs. 4 and 5 reveals an important difference between the two: the C(1*s*) spectrum peaks at 285.8 eV on the {011}-faceted surface, but at 284.7 eV on the {114}-faceted surface. Even with the noise level in these spectra, this 1-eV shift in peak position is unambiguous and suggests that the acetaldehyde-derived adlayer at 310 K is significantly different on the two surfaces. The position of the principal C(1*s*) peak on the {114}-faceted surface, 284.7 eV, is well below even the lowest binding-energy peak, 285.3 eV, in the ethoxide envelope, and thus indicates that the population of ethoxides on the {114}-faceted surface is substantially lower than on the {011}-faceted surface. This is entirely consistent with the TPD results; ethanol is the dominant product in acetaldehyde TPD on the 750 K-annealed surface, but is barely detectable from the 950 K-annealed surface.

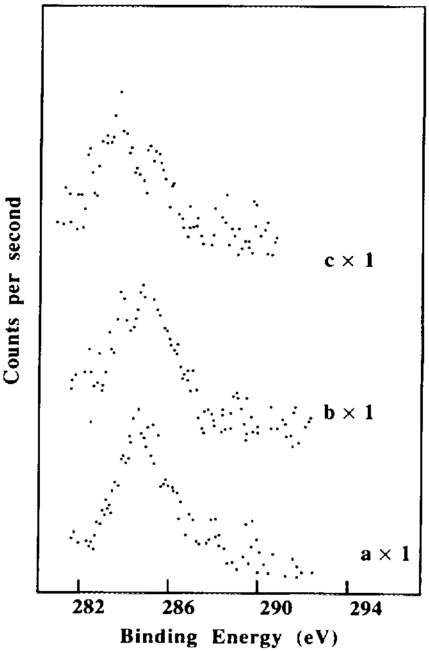

FIG. 5. C(1*s*) spectrum of acetaldehyde on the surface of the {114}-faceted $TiO_2(001)$ single crystal as a function of reaction temperature. (a) 310 K, (b) surface in (a) heated to 450 K, (c) surface in (b) heated to 600 K.

The 284.7-eV peak in Fig. 5a must therefore be associated with the principal reaction products (or surface intermediates from which they are formed), i.e., those of aldol condensation, on the {114}-faceted surface. Candidate species include the intermediate C_2 enolate (CH_2CHO) and C_4 intermediates and products such as crotonaldehyde ($CH_3CHCHCHO$) and crotoxide ($CH_3CHCHCH_2O$) species. As noted above, the enolate would be expected to give rise to C(1*s*) features at binding energies lower than those of alkyl or alkoxide ligands. The sp^2 carbons of the C_4 species would also be expected to exhibit C(1*s*) binding energies lower than those of sp^3 carbons in the alkyl groups of adsorbed acetaldehyde or ethoxide ligands (*46*). Thus the C(1*s*) spectrum of Fig. 5a is quite consistent with the high selectivity to aldol products observed in TPD experiments, but is clearly inadequate for distinguishing between the various surface intermediates along this reaction path. Indeed the spectrum likely contains contributions from several such intermediates. Heating the surface to 450 K, Fig. 5b, decreased the intensity of the C(1*s*) spectrum as expected. Further heating to 600 K clearly removed the majority of the surface species; only two small peaks remained at 285.2 and 284 eV, attributed to C(1*s*) signals of traces of butene (butene has a desorption peak at 500–650 K, Fig. 4) and of surface carbon, respectively.

Two important observations emerge from comparison of Figs. 4 and 5 as well as from the comparison between XPS and TPD results.

1. As clearly demonstrated in Figs. 4 and 5, the C(1*s*) signal corresponding to alkoxide formation (C–O at 286.2 eV) on the 950 K-annealed surface was considerably smaller than that on the 750 K-annealed surface (Fig. 5a compared to Fig. 4b). These results agree well with TPD results for acetaldehyde, showing that ethanol was a major product on the 750 K-annealed surface but that only traces of ethanol were formed on the 950 K-annealed surface.
2. In all cases carboxylate formation (–COO at ca. 289.5 eV) was very small, indicating that the $TiO_2(001)$ single crystal is inactive for aldehyde oxidation in vacuum. In contrast, as indicated by TPD, it is very active for aldolization.

Temperature-Programmed Desorption after Acetaldehyde Adsorption on Titania (Anatase) Powder

Figure 6 presents the product distribution after acetaldehyde adsorption at room temperature on TiO_2 powder (anatase, pretreated in He at 800 K for 2 h). Three product channels were observed. The first at 380 K consisted mainly of acetaldehyde and the second, at 430 K, of crotonaldehyde and crotyl alcohol as well as acetaldehyde. At ca. 550 K a small, broad peak, likely including two different desorption processes at ca. 500 and 600 K was observed. The fragmentation pattern of this minor product appeared to be that of butadiene rather than that of butene observed on $TiO_2(001)$ single-crystal surfaces (Figs. 1 and 2). Crotonaldehyde, the product formed by aldol condensation and dehydration of acetaldehyde, was produced with selectivity of 68% (Table 3), more than three times higher than was observed on either of the single-crystal surface structures. Ethanol production was almost negligible on the powder. In general these results are closer to the 950 K-annealed surface than to the 750 K-annealed surface (more aldolization and only traces of ethanol). This apparent analogy between the 950 K-annealed surface and titania powder has a precedent; acetone was formed by carboxylate coupling on the 950 K-annealed surface ({114}-faceted) surface and on titania powder, but not on the 750 K-annealed surface ({011}-faceted) surface of the $TiO_2(001)$ single crystal (*2*). Thus the broader distribution of coordination environments on the {114}-faceted surface provides a better model for surfaces of polycrystalline materials.

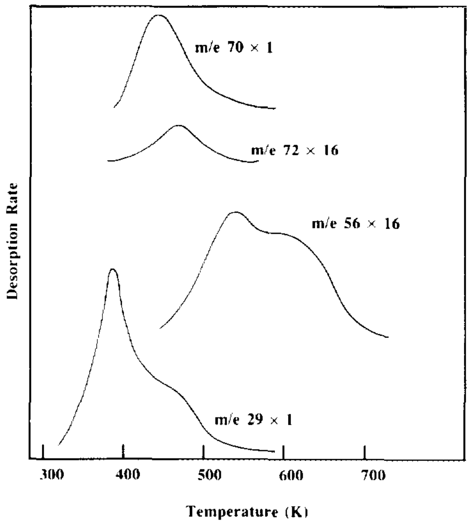

FIG. 6. Product desorption (uncorrected for mass spectrometer sensitivity) after acetaldehyde adsorption at room temperature on TiO_2 powder (anatase).

Table 4 presents the selectivity to C_4 alde-

TABLE 4

Product Selectivity during Acetaldehyde TPD from $TiO_2(001)$ Single-Crystal Surfaces ({011}-Faceted and {114}-Faceted) and TiO_2 Powder

Product	{011}-faceted	{114}-faceted	Powder
Crotonaldehyde	0.19	0.20	0.68
Crotyl alcohol	0.14	0.39	0.07
$\Sigma C_4(O)/\Sigma C_2(O)$	0.5	1.5	3.75

hydes and C_4 alcohols and the ratio of C_4 oxygenates/C_2 oxygenates (denoted as $C_4(O)/C_2(O)$) on the surfaces of the TiO_2 single crystal and powder. Crotyl alcohol was formed with relatively high yield on the surface of the single crystal, particularly on the 950 K-annealed surface. Titania powder was the most active and selective for aldolization to crotonaldehyde; the ratio $C_4(O)/C_2(O)$ was 3.75 for titania powder, more than twice that of the 950 K-annealed surface and ca. seven times higher than that of the 750 K-annealed surface.

DISCUSSION

The reactions of acetaldehyde on the surfaces of the titania single crystal and powder can be summarized as follows.

1. Aldolization

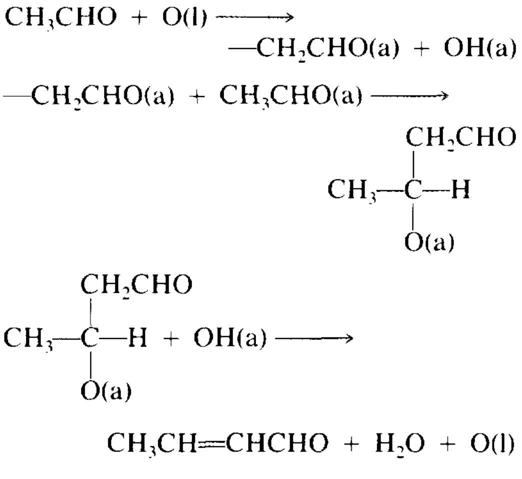

$$CH_3CHO + O(l) \longrightarrow -CH_2CHO(a) + OH(a)$$

$$-CH_2CHO(a) + CH_3CHO(a) \longrightarrow CH_3-\underset{O(a)}{\overset{CH_2CHO}{C}}-H$$

$$CH_3-\underset{O(a)}{\overset{CH_2CHO}{C}}-H + OH(a) \longrightarrow CH_3CH{=}CHCHO + H_2O + O(l)$$

The abstraction of a proton in the α position of the aldehyde by lattice oxygen O(l) would result in the formation of a surface hydroxyl OH(a) and a $-CH_2CHO(a)$ species. $-CH_2CHO(a)$, a nucleophilic species, can react with the electrophilic carbonyl group of second adsorbed acetaldehyde molecule to give adsorbed aldol. The reaction of the aldol with surface hydroxyls to produce net dehydration gives crotonaldehyde ($CH_3CH{=}CHCHO$) and water and restores the lattice oxygen consumed in the first step. Although the selectivity to this α,β unsaturated C_4 aldehyde was different on the three surfaces investigated, it is important to note that significant extents of aldolization were observed on all surfaces.

2. Reduction of Aldehydes to Alcohols

Reduction of acetaldehyde to ethanol

$$CH_3CHO(a) + H(a) \longrightarrow CH_3CH_2O(a)$$

$$CH_3CH_2O(a) + OH(a) \longrightarrow CH_3CH_2OH + O(l)$$

A small fraction of the acetaldehyde was totally decomposed to surface carbon, adsorbed hydrogen, and surface oxygen. Adsorbed hydrogen could serve to reduce part of the adsorbed acetaldehyde that did not participate in the aldolization reaction, giving ethoxide species ($CH_3CH_2O(a)$). Ethoxides were protonated by surface hydroxyls to yield ethanol, leaving lattice oxygen. If one represents surface ethoxides in the usual fashion as anionic ligands bond to surface cations, ethoxide formation from acetaldehyde would formally represent hydride addition and ethoxide conversion to ethanol would require proton addition. The surface sites from which hydridic and protonic hydrogens are supplied are taken to be surface metal cations and surface oxygen anions, respectively. Direct evidence for multiple forms of hydrogen on single-crystal oxide surfaces is generally lacking owing to the limited application to date of vibrational spectroscopies capable of distinguishing between these forms.

Reduction of crotonaldehyde to crotyl alcohol

$$CH_3CH{=}CHCHO(a) + H(a) \longrightarrow CH_3CH{=}CHCH_2O(a)$$

$$CH_3CH{=}CHCH_2O(a) + OH(a) \longrightarrow CH_3CH{=}CHCH_2OH + O(l)$$

Crotonaldehyde reduction to crotyl alcohol occurs in the same fashion as acetaldehyde reduction to ethanol. Crotyl alcohol was observed on all three surfaces. It should also be noted that on the two single-crystal surfaces the overall selectivities for aldehyde hydrogenation varied much less than those for individual products: the {011}-faceted surface produced ethanol, but the {114}-faceted surface favored crotonaldehyde hydrogenation to crotyl alcohol at the expense of ethanol formation.

3. Reductive Coupling

$$2CH_3CHO(a) \longrightarrow CH_3CH{=}CHCH_3 + 2O(l)$$

Traces of butene from both surfaces of the single crystal and traces of butadiene from the powder were observed during acetaldehyde TPD. It was previously demonstrated that carbonyl coupling occurs on defect-containing TiO_2 surfaces (*24*); in particular, butene was observed with high selectivity on the sputtered surface of a $TiO_2(001)$ single crystal (*24*, *47*) and its yield decreased as the annealing temperature was increased (i.e., as the oxidation of titanium suboxides to Ti^{4+} by oxygen migration from the bulk to the surface progressed). Thus, olefin formation can be ascribed to acetaldehyde coupling on a small number of defect sites on the TiO_2 surfaces. It may be feasible to utilize the yield of C_4 olefins in acetaldehyde TPD as a diagnostic tool to estimate quantitatively the defect sites on a nominally "stoichiometric" or "fully oxidized" surface. According to TPD results these sites were responsible for the formation of C_4 olefins representing 1, 2, and 5% of the total acetaldehyde adsorbed on the 750 K-annealed $TiO_2(001)$ surface, the 950 K-annealed $TiO_2(001)$ surface, and the TiO_2 powder, respectively.

4. Cannizzaro Reaction

$$CH_3CHO(a) + O(l) \longrightarrow CH_3CHOO(a)$$

$$CH_3CHOO(a) + CH_3CHO(a) \longrightarrow CH_3COO(a) + CH_3CH_2O(a)$$

The Cannizzaro reaction was at best a minor pathway for acetaldehyde on the two single-crystal surfaces. The carboxylate C(1*s*) signals were quite small compared to those corresponding to less oxidized adsorbates, and TPD results did not show evidence for significant carboxylate decomposition (expected to yield CO_2 at ca. 600 K (*2*)). TPD studies on the surface of titania powder showed no evidence for surface acetate decomposition products (CO_2, methane, or acetone), in agreement with single-crystal work.

A comparative summary of the reactivities of acetaldehyde (this work), formaldehyde (*18*, *27*), and higher linear aldehydes (*30*) on the surfaces of titania powder and single crystals can be stated as follows.

1. It was previously reported that the steady-state aldolization of C_3 and C_4 aldehydes to α,β-unsaturated C_6 and C_8 aldehydes, respectively, occurs with high yield (80% conversion and ca. 90% selectivity) on titania (anatase) at 400–500 K (*30*). Our TPD results indicated that 80% of adsorbed acetaldehyde on titania powder (anatase) reacted to give crotonaldehyde (68% yield), crotyl alcohol (7% yield), and butadiene (5% yield). The selectivities to crotonaldehyde, crotyl alcohol, and butadiene are thus 85, 8.8, and 6.3%, respectively. These results are very close to those obtained during steady-state reactions (*30*), especially if one considers that the TPD experiment covers a wide range of temperatures and surface coverages.

2. The Cannizzaro reaction was a minor path compared to aldolization in reactions

of acetaldehyde on the (001) surfaces; this reaction was the main route for formaldehyde consumption on stoichiometric TiO_2 surfaces. This distinction is entirely consistent with the chemistry of these aldehydes in basic solution.

3. The {114}-faceted surface was more selective for aldolization than the {011}-faceted surface (Table 4). Since the {114}-faceted structure contains Ti^{4+} cations in a wider range of coordination environments than the {011}-faceted structure, it appears that the aldolization reaction, while not strongly structure-sensitive, is favored by surface heterogeneity.

Quantitative activity comparisons between single crystals and powders cannot be made from TPD experiments owing to the contributions made by readsorption and possible further reaction of both reactants and products on high-surface-area samples. The same limitation holds for comparison of selectivities to intermediate products if the reaction network is sequential, since selectivity will be a function of conversion. However, for competing *parallel* reactions, e.g., acetaldehyde hydrogenation vs aldolization, product selectivities should be less sensitive to conversion levels and therefore to the effects of readsorption in powder studies. This comparison in the present case serves to illustrate both the distinction between the reactivities of the {011}- and {114}-faceted single-crystal surfaces, and the strong analogy between the more heterogeneous of these, the {114}-faceted surface and the polycrystalline powder.

Eighty percent of the acetaldehyde molecules initially adsorbed reacted to other products in the powder TPD experiments. Conversion of acetaldehyde on the {011}-faceted surface was 70%. Let us assume that by readsorption events the conversion could be increased to 80%, but that the selectivity to ethanol vs aldol products will remain the same for readsorbed acetaldehyde as for the initially adsorbed reactant molecules. The $\Sigma C_4(O)/\Sigma C_2(O)$ ratios for the single-crystal surface appearing in Table 4 can then be extrapolated to higher conversions. For 80% conversion at constant selectivity from the {011}-faceted surface, the value of this ratio would be 0.65. The same analysis applied to extend results from the {114}-faceted surface from 61 to 80% conversion leads to a projected $\Sigma C_4(O)/\Sigma C_2(O)$ ratio for this surface of 4. The measured value on the polycrystalline powder was 3.75, in excellent agreement with the behavior of the {114}-faceted surface, extended to comparable conversions. The ratio for the {011} surface was substantially different, and moreover, the $\Sigma C_4(O)/\Sigma C_2(O)$ ratio for this surface cannot exceed unity even if acetaldehyde is readsorbed and recycled to extinction.

The mechanism by which surface heterogeneity promotes aldol condensation on the single-crystal surfaces is unclear. As noted above, this bimolecular reaction does not *require* fourfold coordinated surface cations; unlike the bimolecular ketonization of carboxylates, aldolization occurs on the {011}-faceted (001) surface of TiO_2. The analogy with base-catalyzed aldol condensation in solution also supports the absence of a requirement for a specific surface coordination environment. Since OH^- in solution is sufficient to catalyze aldol condensation, one would not expect this reaction on a surface to require sites other than the acid–base site pairs needed for heterolytic dissociation.

The increase in aldolization selectivity with increasing surface heterogeneity may simply reflect the influence of the surface on hydrogenation activity. Again the details are unclear. However, we note that since both the aldol condensation and hydrogenation reactions occur readily below ca. 400 K, an increase of only 2 kcal/mol in the hydrogen binding energy or the activation barrier for hydrogenation would be sufficient to change the ratio of aldolization/hydrogenation rates by more than a factor of 10. Such a small variation in the surface–adsorbate bond strength is well within the range of energetic nonuniformity required to explain non-

Langmuirian isotherms for adsorption on polycrystalline oxides (*48*, *49*). Thus the apparent dependence of aldolization selectivity on surface nonuniformity likely reflects the influence of nonuniformity on the competing hydrogenation reaction, rather than an intrinsic surface structural requirement of the aldol condensation itself.

CONCLUSIONS

$TiO_2(001)$ single-crystal surfaces (in UHV) and TiO_2 powder (at 1 atm) were active for aldolization of acetaldehyde. The {114}-faceted surface was more selective than the {011}-faceted surface for aldolization. In no case was the simple aldol product observed; crotonaldehyde and crotyl alcohol (the α,β-unsaturated products) were the principal products. No C=C bond hydrogenation was observed; both titania single crystal and powder samples hydrogenated only the aldehyde function. The Cannizzaro-type disproportionation of acetaldehyde to ethoxides and acetates was found to be a minor route compared to condensation.

ACKNOWLEDGMENT

We gratefully acknowledge the support of the National Science Foundation (Grants CTS 87-14416 and CTS 91-00404) for this research.

REFERENCES

1. Rubinstein, A. M., Yakerson, V. I., and Lafer, L. I., *Kinet. Katal.* **5,** 319 (1964).
2. Kim, K. S., and Barteau, M. A., *J. Catal.* **125,** 353 (1990).
3. Vohs, J. M., and Barteau, M. A., *Surf. Sci.* **201,** 481 (1990).
4. Peng, X. D., and Barteau, M. A., *Catal. Lett.* **7,** 395 (1990).
5. Cunningham, J., Morrissey, D. J., and Goold, E. L., *J. Catal.* **53,** 68 (1978).
6. Kim, K. S., and Barteau, M. A., *Surf. Sci.* **223,** 13 (1989).
7. Kim, K. S., Barteau, M. A., and Farneth, W. E., *Langmuir* **4,** 533 (1988).
8. Rossi, P. F., Busca, G., Lorenzelli, V., Sam, O., and Lavalley, J. C. *Langmuir* **3,** 52 (1987).
9. Bowker, M., Houghton, H., and Waugh, K. C., *J. Catal.* **79,** 431 (1987).
10. Vohs, J. M., and Barteau, M. A., *Langmuir* **5,** 965 (1989).
11. Kiennemann, A., Idriss, H., Kieffer, R. Chaumette, P., and Durand, D., *Ind. Eng. Chem. Res.* **30,** 1130 (1991).
12. Miyata, H., Toda, Y., and Kubokawa, Y., *J. Catal.* **32,** 155 (1974).
13. Vohs, J. M., and Barteau, M. A., *J. Phys. Chem.* **95,** 287 (1991).
14. Bowker, M. Houghton, H., and Waugh, K. C., *J. Chem. Soc. Faraday Trans. I* **71,** 2573 (1982).
15. Vohs, J. M., and Barteau, M. A., *Surf. Sci.* **197,** 109 (1988).
16. Graham-Solomons, T. W., "Organic Chemistry," 3rd ed., p. 738. Wiley, New York.
17. Benat, P., Bertolini, J. C. Gautier, Y., Massardier, J., and Ruiz, P., *J. Catal.* **126,** 451 (1990).
18. Lavalley, J. C., Lamotte, J., Busca, G., and Lorenzelli, V., *J. Chem. Soc. Chem. Commun.*, 1006 (1986).
19. Li, C., Domen, K., Mamiya, K., and Onishi, T., *J. Catal.* **125,** 445 (1990).
20. Ai, M., *J. Catal.* **124,** 293 (1990).
21. Ai, M., *J. Catal.* **107,** 201 (1987).
22. Giancarlo, A., and Moggi, P., *Appl. Catal.* **37,** 315 (1988).
23. Joshi, M. V., and Narasimhan, C. S., *J. Catal.* **128,** 63 (1991).
24. Idriss, H., Pierce, K., and Barteau, M. A., *J. Am. Chem. Soc.* **113,** 715 (1991).
25. Idriss, H., Hindermann, J. P., Kieffer, R., Kiennemann, A., Vallet, A., Chauvin, C., Lavalley, J. C., and Chaumette, P., *J. Mol. Catal.* **42,** 205 (1987).
26. Peng, X. D., and Barteau, M. A., *Langmuir* **5,** 1051 (1989).
27. Idriss, H., Kim, K. S., and Barteau, M. A., *Surf. Sci.* **262,** 113 (1992).
28. Vohs, J. M., and Barteau, M. A., *Surf. Sci.* **176,** 91 (1986).
29. Morrison, R. T., and Boyd, R. N., "Organic Chemistry," 5th ed., p. 913. Allyn & Bacon, Rockleigh, NJ, 1987.
30. U.S. Patent, 4,316,990 (1982).
31. Zhang, G., Hattori, H., and Tanabe, K., *Appl. Catal.* **36,** 189 (1988).
32. Dabbagh, H., and Davis, B., *J. Mol. Catal.* **48,** 117 (1988).
33. U.S. Patent, 3,948,991 (1972).
34. German Patent, 2,505,580 (1976).
35. Idriss, H., Libby, M., and Barteau, M. A., unpublished results.
36. Hayes, R. N., Grese, R. P., and Gross, M. L., *J. Am. Chem. Soc.* **111,** 8336 (1989).
37. Baigri, L. M., Cox, R. A., Slebocka-Tilk, H., Tencer, M., and Tidwell, T. T., *J. Am. Chem. Soc.* **107,** 3640 (1985).
38. Denmark, S. E., and Hanke, B. R., *J. Am. Chem. Sco.* **113,** 2177 (1991).
39. Hoflund, G. B., Yin, H. L., Grogan, Jr., A. L.

Asbury, D. A., Yoneyama, H., Ikeda, O., and Tamura, H., *Langmuir* **4,** 346 (1988).

40. Firment, L. E., *Surf. Sci.* **116,** 205 (1982).

41. Madix, R. J., Yamada, T., and Johnson, S. W., *Appl. Surf. Sci.* **19,** 43 (1984).

42. Ko, E. I., Benziger, J. B., and Madix, R. J., *J. Catal.* **62,** 264 (1980).

43. Bakke, A. A., Chen, H. W., and Jolly, W. L., *J. Electron Spectrosc. Relat. Phenom.* **20,** 333 (1983).

44. Vohs, J. M., Ph.D. dissertation, University of Delaware, 1988.

45. Kim, K. S., and Barteau, M. A., *J. Mol. Catal.* **63,** 103 (1990).

46. Vohs, J. M., and Barteau, M. A., *J. Phys. Chem.* **93,** 8343 (1989).

47. Idriss, H., Libby, M., and Barteau, M. A., *Catal. Lett.*, **15,** 13 (1992).

48. Boaventura, J. S., Ph.D. dissertation, University of Delaware, 1989.

49. Spitz, R. N., Barton, J. E., Barteau, M. A., Staley, R. H., and Sleight, A. W., *J. Phys. Chem.* **90,** 4067 (1986).